

## Effect of Titanium Dioxide Nanogel Surface Charges and Particle Size on Anti-Corrosion Performances of Epoxy Coatings

Ayman M. Atta<sup>1,2,\*</sup>, Hamad A. Al-Lohedan<sup>1</sup>, Ashraf M. El-saeed<sup>2</sup>, Ahmed M. Tawfeek<sup>3</sup> and Mohamed H. Wahby

<sup>1</sup> Chemistry Department, College of Science, King Saud University, Riyadh 11451, Saudi Arabia.

<sup>2</sup> Petroleum application department, Egyptian petroleum research institute, Nasr city 11727, Cairo, Egypt.

<sup>3</sup> College of Science, King Saud University, Riyadh 11451, Saudi Arabia.

\*E-mail: [khaled\\_00atta@yahoo.com](mailto:khaled_00atta@yahoo.com)

Received: 3 November 2016 / Accepted: 11 December 2016 / Published: 30 December 2016

---

The relationship between surface charges and particle sizes of nanomaterials and their effects on the anticorrosion performance of epoxy organic coatings are not previously reported. Herein, the interfacial potential and size dependent of titanium dioxide (TiO<sub>2</sub>) nanogel composite is investigated by changing the particle charges. In this respect commercially available TiO<sub>2</sub> nanoparticles are used as core to form nanogel composites based on 3-acrylamidopropyl) trimethylammonium chloride (APTAC) using radical crosslinking free surfactants solution polymerization. The surface charges of nanogel composites were changed by using co-monomer with APTAC such as acrylic acid (AA), N-isopropyl acrylamide (NIPAm) and 2-acrylamido-2-methylpropane sulfonate sodium salt (AMPS-Na). The particle size, surface morphology and thermal stability of TiO<sub>2</sub> nanogel composite were determined. The surface charges and their variation with pH of TiO<sub>2</sub> aqueous nanogel composite solutions were investigated. TiO<sub>2</sub> nanogel composites were embedded in epoxy coatings with different concentrations to investigate the effect of their surface charges, particle size and dispersability on anticorrosion performances of epoxy coatings in aqueous salt solutions.

---

**Keywords:** corrosion; TiO<sub>2</sub> nanogel composite; salt spray; epoxy organic coatings; steel.

### 1. INTRODUCTION

The epoxy resins as thermoset organic polymers have been widely used as structural polymer composites, adhesive, paints, automotive and electronic industries [1-3]. Cured epoxy resins have great advantages over other organic coatings to apply as primer coatings due to their excellent adhesion, thermal, anticorrosion performances and the easy processing under different conditions [4].

One of great disadvantage raised from exothermic curing reaction of highly crosslinked epoxy matrix is brittleness and microcracks that change the epoxy coating performances [5]. Nano-fillers attracted great attention to reinforce epoxy matrix during curing process [6-9]. These materials can be blended with epoxy matrix with low concentrations due to their unique properties. The challenges to apply these materials are based on toxicity, dispersability and homogeneity in epoxy matrix due to their high reactivity. Due to these excellent properties that enhance the coating performance, metal oxides such as  $\text{TiO}_2$  is more interesting nanomaterials that has non-toxicity and high resistance to chemicals, corrosion and weather durability due to its affinity to absorb ultraviolet (UV) light [10-12]. The  $\text{TiO}_2$  nanoparticles were used to reinforce the mechanical properties of epoxy resins but they have limited due to their low dispersability in epoxy matrix [13]. It was proposed that high-energy ball milling process used to improve the dispersability of nanoparticles in different polymer matrixes [14]. Mostly, the dispersion of nanoparticles in polymer matrix can be enhanced by the ultrasonic that affected by degradation of nanomaterials, cluster size, surface charges and types of nanomaterials [15, 16].

Among several strategies proposed to increase the dispersion of nanomaterials in the polymer matrixes such as melt processing [17, 18], chemical modification of nanomaterial surfaces [19, 20] or polymer matrix modification [21] proposed as favorable techniques to improve the dispersability of nanomaterials. In the present work, the chemical modifications of nanomaterials to change their surface charges is proposed as new technique to improve the nanomaterial dispersability in epoxy matrix. It is well known that, the particles required charges at their surfaces to disperse in liquids. Moreover, it was previously reported that the surface charges of  $\text{TiO}_2$  nanoparticles could be affected by the size of these particles [22]. The literature survey confirmed that there is relatively little information that correlated between particle surface charge and its size distribution. For these purposes the present work has been planned to produce homogeneously dispersed  $\text{TiO}_2$ -nanogel epoxy composites having different zeta potentials values and charges to investigate new relationship between surface charges and corrosion inhibition efficiency of  $\text{TiO}_2$ -nanogel epoxy composites as organic coat for steel. The influence of  $\text{TiO}_2$  nanogel contents in epoxy matrix and their dispersion condition on mechanical properties of epoxy matrix has been investigated.

## 2. EXPERIMENTAL

### 2.1. Materials

The chemicals used in this work are purchased from Aldrich Sigma Company. Titanium dioxide ( $\text{TiO}_2$  nano-powder with average particle size 21 nm) was used as core for nanogel. 3-Acrylamidopropyl trimethylammonium chloride (APTAC), acrylic acid (AA), N-isopropyl acrylamide (NIPAm) and 2-acrylamido-2-methylpropane sulfonate sodium salt (AMPS-Na) were used to prepare copolymeric nanogel based on APTAC. *N,N*-Methylenebisacrylamide (MBA chemical crosslinker), ammonium persulfate (APS radical initiator), *N,N,N',N'*-tetramethylethylenediamine (TEMED activator) and poly(vinyl pyrrolidone) (PVP with molecular weight 40,000 g/mol as dispersing agent) were reacted without purification. SigmaGuard™ CSF 650 (produced by Sigma

Coatings SigmaKalon Group) was used as commercial epoxy organic coatings after mixed with its polyamide hardener by volume 4:1.

The TiO<sub>2</sub> nanogel composites were synthesized in our previous works [23, 24]. The crosslinking copolymerization of APTAC with AA or AMPS-Na or NIPAm with mol ratio of 50/50 for each monomer using 10 mol% of MBA crosslinker, 10 mmol of TEMED and 0.1 Wt % of APS was carried out after dissolving the mixture of ethanol/water (60/40 Vol %). This mixture was added to dispersion solution of TiO<sub>2</sub> powder (1g) in 100 mL of and PVP (1 g) under vigorous stirring. The reaction temperature was increased up to 55 °C to complete the polymerization. The isolation of nanogel and its purification was carried out according to previous work [23, 24].

## 2.2. Preparation of epoxy/ TiO<sub>2</sub> nanocomposites coatings

TiO<sub>2</sub> nanogel composites of APTAC/ AA, APTAC/NIPAm and APTAC/ AMPS-Na were mixed with polyamide hardener at different weigh ratios ranged from 0.1 to 3 wt.% using ultrasonication rod to complete nanogel powder dispersion. The dispersed solution of TiO<sub>2</sub> nanogel composites polyamide hardener was mixed with epoxy resin according to recommended volume ratio. The mixture air sprayed on the blasted and cleaned steel panels to form thickness of 100 µm to cure and test after 7 days. The blank sample was prepared after mixing epoxy with hardener without adding TiO<sub>2</sub> nanogel composites.

## 2.3. Characterization

The TiO<sub>2</sub> and nanogel contents into composite were determined using thermogravimetric analysis (TGA; TGA-50 SHIMADZU at flow rate 50 ml/min and heating rate of 20 °C/min).

The morphology of TiO<sub>2</sub> nanogel composites was studied using high resolution transmission electron microscope (HR-TEM using a JEOL JEM-2100 electron microscope at an acceleration voltage of 200 kV).

The solution properties of dispersed TiO<sub>2</sub> nanogel composites such as zeta potential, particle diameter, polydispersity index (PDI) were recorded by dynamic light scattering (DLS using Laser Zeta meter Malvern Instruments; Model Zetasizer 2000).

The surface morphology of TiO<sub>2</sub> nanogel composites embedded into epoxy coatings was investigated using high resolution scanning electron microscope (SEM using a JEOL JEM-2100).

## 2.4. Mechanical Properties of epoxy/ TiO<sub>2</sub> nanocomposites coatings

The preparation of the steel panels and assessment of mechanical properties such as impact resistance, hardness, T-bending and pull-off resistance were tested according to ASTM methods. Hydraulic pull-off adhesion tester (DeFelsko PosiTest digital Pull-Off adhesion tester has force ranged 0–25 MPa with 20 mm dollies) was used to evaluate the adhesion pull-off resistance according to ASTM D4541. Erichsen hardness test pencil (model 318S has scratching force ranged from 0.5 to 20

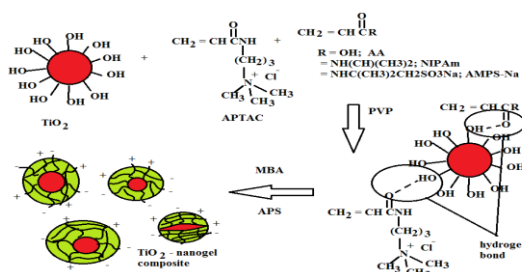
N) was used to evaluate the hardness of cured films. TABER® Rotary platform abrasion tester (Model 5155) was used to determine the abrasion resistance of cured epoxy films according to ASTM D4060-07 after using load of 1Kg and rotation of 5000 cycle on the epoxy coated steel panels.

#### 2.4. Salt spray resistance of epoxy/TiO<sub>2</sub> nanocomposites coatings

Salt spray resistance test of damaged epoxy nanocomposites on steel panels carried out according to ASTM- B117 was used to evaluate their corrosion resistances to salt and humidity. A salt spray cabinet (manufactured by CW Specialist equipment ltd. model SF/450) recommended to carry the test at different time intervals up to 1000 h.

### 3. RESULTS AND DISCUSSION

The present work aims to prepare crosslinked polyelectrolyte and polyampholyte nanogel composites based on TiO<sub>2</sub> to investigate the effect of surface charges of the nanomaterials on the dispersion and corrosion inhibition as organic coatings for steel. In this respect the polyampholyte nanogels, contain both negative and positive charges in the polymer chains, were prepared by radical crosslinking copolymerization of APTAC with AMPS-Na or AA. The stimuli-responsive polyelectrolyte nanogel was prepared by using NIPAm and APTAC to form crosslinked copolymer in the presence of MBA as crosslinker. In our previous works [23, 24], TiO<sub>2</sub> nanogel composites were successfully prepared in the presence of PVP as stabilizer and ethanol/water (60/40 Vol %) as dispersion co-solvent. The Scheme of reaction is represented in scheme 1 to confirm that the interaction between TiO<sub>2</sub> and amide groups of monomers (APTAC, AA, and AMPS-Na) facilitates the formation of core/shell TiO<sub>2</sub> nanogel composites. It is expected that the repulsion or attraction between negative charge of TiO<sub>2</sub> with AA, AMPS-Na or APTAC can affect the surface charges, particle size and their dispersion in epoxy matrix or polar solvents.



**Scheme 1.** Preparation route of TiO<sub>2</sub> Nanogel composites.

#### 3.1. Characterization

The surface morphologies of the prepared TiO<sub>2</sub> and their nanogels with APTAC/NIPAm, APTAC/AMPS-Na and APTA/AA are used to evaluate the interactions between charged

nanoparticles. In this respect, the TEM micrographs of  $\text{TiO}_2$  and their nanogels with APTAC/NIPAm, APTAC/AMPS-Na and APTA/AA are illustrated in Figure 1 a-d. The connected spherical particles with size 15-25 nm for  $\text{TiO}_2$  nanoparticles (Figure 1 a) confirms the lower dispersion of  $\text{TiO}_2$  in water beside that particles can attract to each other due to their lower surface charges. The dispersion of  $\text{TiO}_2$  nanoparticles into APTAC/AMPS-Na (Figure 1 b) and appearance of shadow black spherical nanogel elucidates the encapsulation of nanogel particles with  $\text{TiO}_2$ . The dispersion of particles confirms that there are repulsive forces and higher surface charges on the  $\text{TiO}_2$ - APTAC/AMPS-Na nanogel particles. The formation of  $\text{TiO}_2$  cluster inside nanogel composites based on APTAC/NIPAm (Figure 1 c) indicates the interaction between  $\text{TiO}_2$  and nanogel networks and formation of core/shell morphologies. Moreover, the formation of low thick film of nanogel based on APTA/AA to surround the  $\text{TiO}_2$  nanoparticle as core is elucidated from Figure 1d. It was also observed that all  $\text{TiO}_2$  nanoparticles are surrounded by nanogel to form composites. These data confirm that the interaction between  $\text{TiO}_2$  and nanogels affect the degree of encapsulation of  $\text{TiO}_2$  inside the nanogel networks [25].

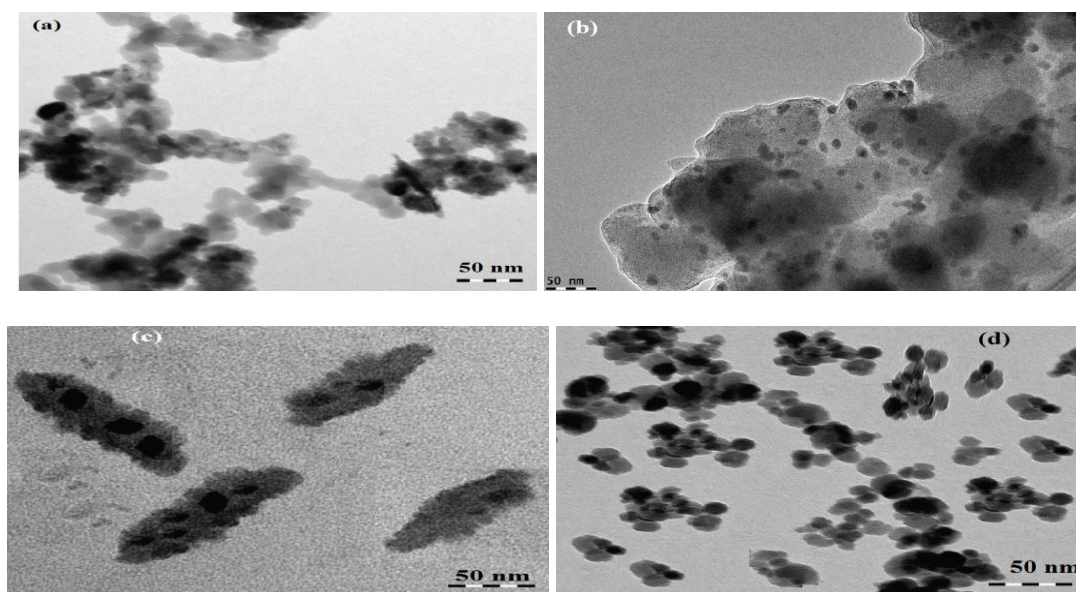


**Figure 1.** TEM micrographs of a)  $\text{TiO}_2$ , b)  $\text{TiO}_2$ -APTAC/AMPS-Na, c)  $\text{TiO}_2$ -APTAC/NIPAm and d)  $\text{TiO}_2$ -APTAC/AA nanogel composites.

It is very important to determine the quantity of  $\text{TiO}_2$  encapsulated inside the nanogel networks as using TGA data summarized in Table 1. The presence of hydroxyl groups surrounded to  $\text{TiO}_2$  (scheme 1) is confirmed from the weight losses of 4 % from  $\text{TiO}_2$  original weight below  $250^\circ\text{C}$  due to dehydration of the water at this temperature range (Table 1). This percentage at temperature ranged from 25 to  $250^\circ\text{C}$  is increased with incorporation of nanogel and increasing the nanogel hydrophilicity in the order APTAC/AMPS-Na > APTAC/AA > APTAC/NIPAm as represented in Table 1. It was also noticed that the quantity of water loss increased with the incorporation of NIPAm/AA more than NIPAm/AAm due to the strong hydrophilicity of NIPAm/AA networks. The decomposition of

nanogels from 250 to 550 °C was increased in the nanogels contain APTAC/NIPAm and APTAC/AMPS-Na more than that contains APTAC/AA due to losses of ammonia gas at low temperature more than decarboxylation of AA due to a large-scale oxidative thermal decomposition of network chains [27]. TGA data (Table 2) elucidate that the TiO<sub>2</sub> contents increased in the order APTAC/AA > APTAC/NIPAm > APTAC/AMPS-Na which agree with the TEM micrographs (Figure 1a – d). This means that there is strong intra- molecular interactions between hydroxyl groups of TiO<sub>2</sub> and amide groups of AMPS-Na more than COOH groups of AA due to repulsive forces between charged sulfonate groups.

**Table 1.** TGA data of amphiphilic titanium dioxide nanogel composites.

TiO <sub>2</sub> Nanogels modifier	Remaining		TiO <sub>2</sub> contents (Wt%)
	Temperature range °C	Weight loss (Wt%)	
TiO <sub>2</sub>	25-250	4	96
	250-550 °C	0	
	550-750 °C	0	
APTAC/AMPS-Na	50-250	8	50
	250-550	40	
	550-750	2	
APTAC/NIPAm	50-250	5	60
	250-550	33	
	550-750	2	
APTAC/AA	50-250	6	68
	250-550	23	
	550-750	3	

The surface charge of nanoparticles is very important that used to determine the industrial application of nanomaterials [28] which can be determined by measuring the zeta potential as illustrated in Figure 2 and summarized in Table 2. The double layer of charge or zeta potential of nanoparticles in the solution is very important parameter beside particle sizes and dispersability of nanomaterials to apply these materials to prevent their aggregations which inhibit their activity as nanomaterials. In this respect, the particle sizes of TiO<sub>2</sub> nanogels and PDI values were determined and listed in Table 2.

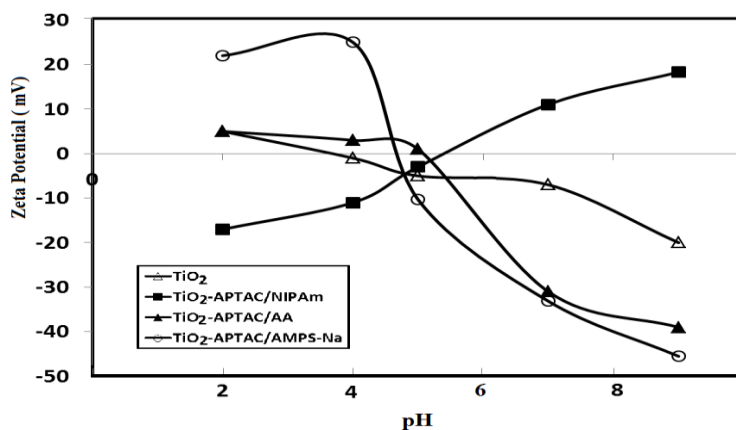


**Figure 2.** Relationship between zeta potential and pH of aqueous dispersed solutions of TiO<sub>2</sub> nanogel composites.

**Table 2.** DLS data of TiO<sub>2</sub>-nanogel composites.

TiO <sub>2</sub> nanogels	pH of isoelectric point	DLS		*Zeta Potential (mV)
		Particle size(nm)	PDI	
TiO <sub>2</sub>	3.8	23 ± 15	1.53	-7.14 ± 5
APTAC/AMPS-Na	4.8	93 ± 5	0.431	-33.13 ± 4
APTAC/AA	5.1	65 ± 15	0.273	-31.27 ± 3
APTAC/NIPAm	5.3	75 ± 8	0.13	11.13 ± 7

\*The all measurements were carried out in 10<sup>-3</sup> M KCl at pH 7.

The pH isoelectric point, pH at zero potential, can be determined from zeta potential measurements at different pH as represented in Figure 3. The correlation between particle sizes (nm) and zeta potential at pH 7 confirms that the surface charges increased with increment of particle sizes of TiO<sub>2</sub> nanogel composite as confirmed for TiO<sub>2</sub>- APTAC/AMPS-Na which has particle size of 93.0 ± 15 nm and zeta potential of -33.13 ± 5 mV (Table 2).

This means that the TiO<sub>2</sub>- APTAC/AMPS-Na the highly charged particles even at low pH cannot form aggregates due to repulsive forces between the same charged particles [29]. The surface charge values are increased in the direction of TiO<sub>2</sub>- APTAC/AMPS-Na > TiO<sub>2</sub>- APTAC/AA > TiO<sub>2</sub>- APTAC/NIPAm which have the same order of lowering particle sizes. The PDI of particles showed reverse order. These mean that the size of TiO<sub>2</sub>- APTAC/NIPAm nanocomposites, having low surface charges, are more uniform than TiO<sub>2</sub>- APTAC/AMPS-Na.

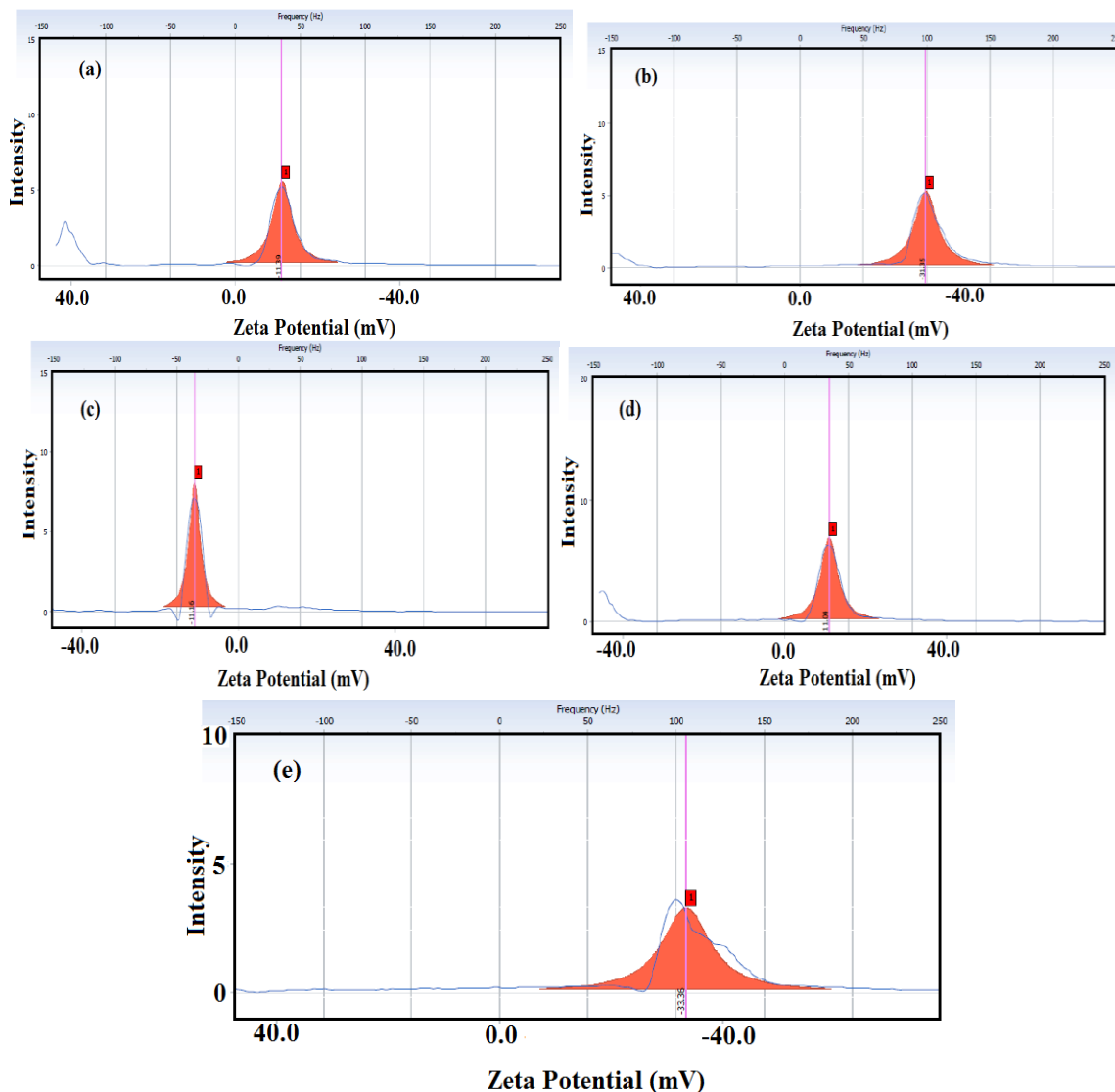


**Figure 3.** Zeta potential of TiO<sub>2</sub>-APTAC/AA at pH a) 4, b) 7, TiO<sub>2</sub>-APTAC/NIPAm c) 4, d) 7 and TiO<sub>2</sub>-APTAC/AMPS-Na e) pH 7.

This behavior can be attributed to electrostatic attraction between anions and cations of polyampholyte TiO<sub>2</sub>-APTAC/AMPS-Na networks which did not found in polyelectrolyte TiO<sub>2</sub>-APTAC/NIPAm networks [30]. Careful inspection of data (Table 2 and figure 3) elucidates that there are more free hydroxyl groups on the TiO<sub>2</sub>-APTAC/AMPS-Na nanocomposites which have low isoelectric point at pH 4.3 [31]. These data elucidates that the modified TiO<sub>2</sub> nanoparticles have different values and signs for zeta potential (Table 2) which reflect on the application of these nanomaterials as filler for epoxy matrix which possess positive charges [32].

### 3.2. Curing and mechanical properties of epoxy TiO<sub>2</sub> nanogel composites

Epoxy resins can be cured with polyamides, polyamines, anhydrides to form thermoset polymers to apply as adhesive and coatings to protect several substrates from corrosion. There are



some microholes or microcracks are produced from heat curing exotherms or due to the physical force interactions such as van der Waals occurred between the epoxy matrix and which forms a channel affected the coat performances as anticorrosive coatings.

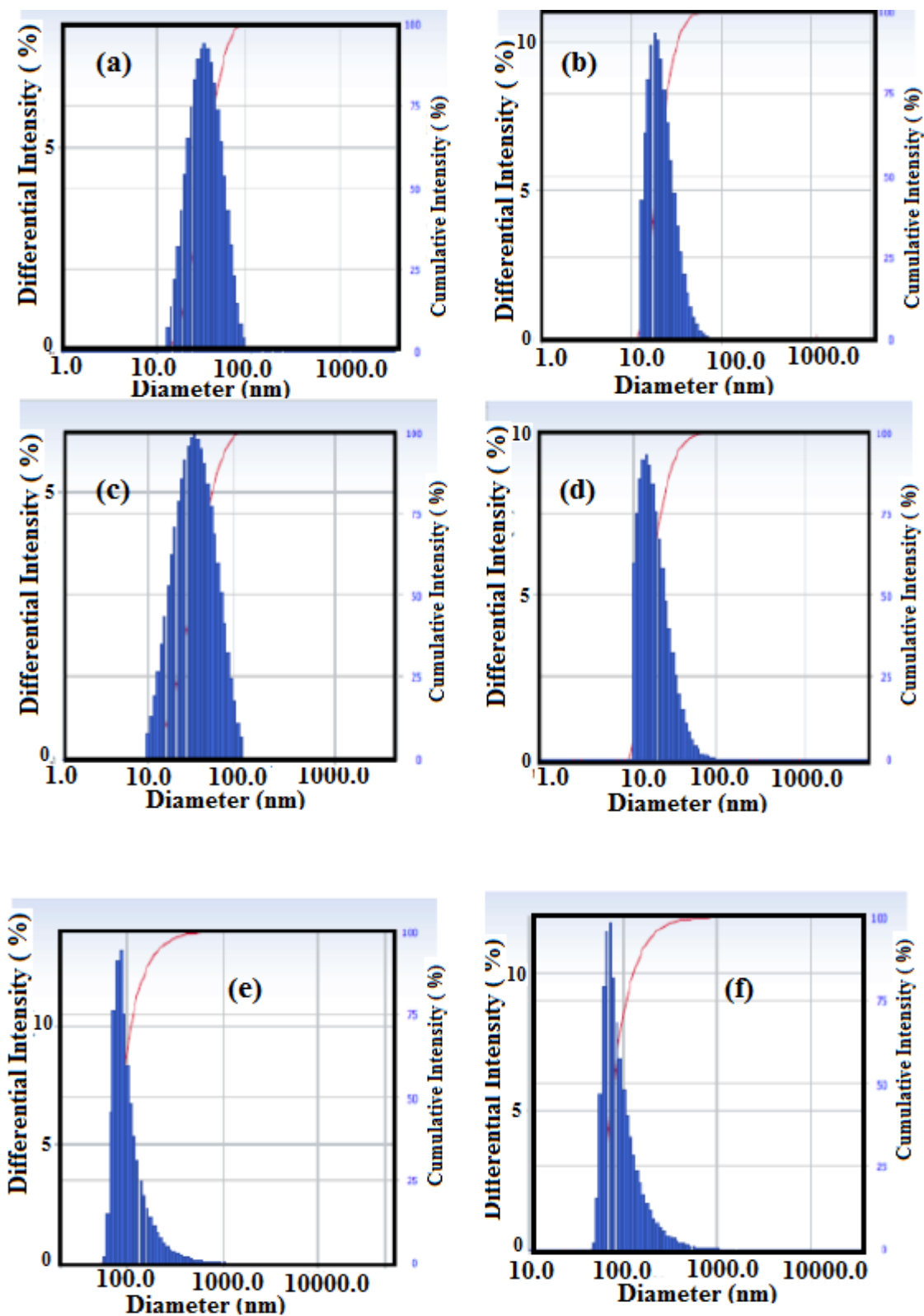


**Figure 4.** Particle size measurements of a), b) TiO<sub>2</sub>-APTAC/AA, c), d) TiO<sub>2</sub>-APTAC/NIPAm and e, f) TiO<sub>2</sub>-APTAC/AMPS-Na in polyamide hardener and water, respectively.

The dispersability of additives in epoxy matrix is the most important parameter that used to overcome the formation of cracks or holes. Nanomaterial based on titanium was used as additives to enhance the anticorrosion performance of epoxy resins [33]. In the present work,  $\text{TiO}_2$  nanogel composites are used as additives for epoxy matrix. The  $\text{TiO}_2$  nanogel composites having different weight percentages ranged from 0.1 to 3.0 (Wt. % based on total weight of epoxy resin and hardener) are dispersed in polyamide that used as hardener as illustrated in the experimental section. DLS measurements for dispersion of  $\text{TiO}_2$  nanogel composites in water and polyamide hardener are represented in Figure 4 a-f. The data confirm that the PDI values and particle size diameters are reduced at dispersion of  $\text{TiO}_2$  nanogel composites in polyamide hardener than water. This means that there strong interaction between amide groups of hardener and nanogel composites by ionic interaction beside the formation of hydrogen bonds between amide groups and free hydroxyl groups on the  $\text{TiO}_2$  surface.

SEM images can be used to investigate the dispersion of  $\text{TiO}_2$  nanogel composites in cured epoxy matrix as represented in Figure 5 a-d.

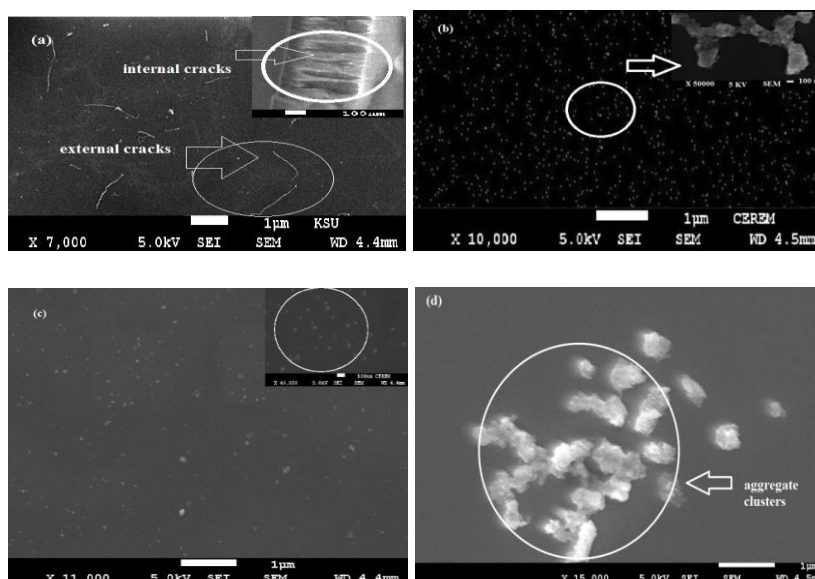
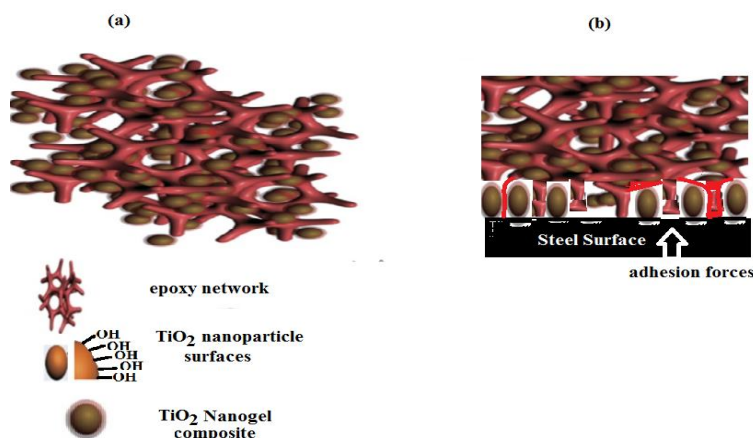


**Figure 5.** SEM micrographs of epoxy surfaces a) blank, b) embedded with  $\text{TiO}_2$ -APTAC/AMPS-Na (0.1 Wt %), c) embedded with  $\text{TiO}_2$ -APTAC/NIPAm (1.0 Wt %) and d) embedded with  $\text{TiO}_2$ -APTAC/AA (3 Wt %).

The blank samples of cured epoxy resins without  $\text{TiO}_2$  nanogel composites (Figure 5 a) shows holes and microcracks at the epoxy coat surfaces. The dispersion of  $\text{TiO}_2$ -APTAC/AMPSA-Na are reduced with increment of its contents from 0.1 to 3.0 Wt % as confirmed from Figure 5 b-d. SEM photos confirm the formation of a well-connected  $\text{TiO}_2$  nanogel with three dimensional epoxy network structure that facilitate their dispersion in the epoxy matrix as represented in Scheme 2. The epoxy network can be bonded with the  $\text{TiO}_2$  nanogel surface via either hydrogen bonding with or polar interactions between charged surfaces of  $\text{TiO}_2$  nanogel and hydroxyl or amide groups of cured epoxy matrix to coat porous space for volume expansion of cured epoxy surfaces. It was expected that the

titanium atoms have 3d empty orbit can be easily bonded with p orbit of active oxygen atoms of hydroxyl groups of cured epoxy curing providing enough active oxygen atoms with electrons to form p-d conjugative effect [34].



**Scheme 2.** Interaction between TiO<sub>2</sub> nanogel and epoxy matrix a)in bulk and b) at steel surface.

It is important to investigate the relation between surface charges or zeta potential of nanoparticles and the adhesion of epoxy resins with steel substrate using pull-off resistance tester as listed in Table 3. The data confirm the increment of adhesion between epoxy composites with increment of TiO<sub>2</sub>-APTAC/AA or TiO<sub>2</sub>-APTAC/AMPS-Na contents and steel substrate. The incorporation of TiO<sub>2</sub>-APTAC/NIPAm into epoxy matrix did not show any significant improvement in adhesion values.

**Table 3.** Mechanical properties of TiO<sub>2</sub>-nanogel epoxy films.

TiO <sub>2</sub> nanogel	Nanogel content (Wt %)	Impact test (Joule)	Hardness (Newton)	abrasion resistance mg / 1kg weight for 5000 cycles	Pull of test (MP)
Blank		11	8	72	5
APTAC/NIPAm	0.1%	13	11	27	7
	1%	15	12	23	6
	3%	14	12	23	5
APTAC/AA	0.1%	13	11	19	10
	1%	13	11	32	12
	3%	12	11	31	9
APTAC/AMPS-Na	0.1%	14	12	19	12
	1%	15	13	19	15
	3%	17	14	24	8

The increment of TiO<sub>2</sub> nanogel composites contents reduces the adhesion strength values as listed in Table 3. These data can be referred to the increment of attraction forces between the negative charges on the surfaces of TiO<sub>2</sub>-APTAC/AA or TiO<sub>2</sub>-APTAC/AMPS-Na ( Table 2) and positive charges of steel which alters by nanogel accumulation [32, 35]. Moreover, the repulsive forces between positive charges of TiO<sub>2</sub>-APTAC/NIPAm and steel surfaces reduce the adhesion strength between epoxy and steel surfaces. The improvement of mechanical properties of TiO<sub>2</sub> nanogel composites such as impact resistance, hardness and abrasion resistance (Table 2) confirms the good interactions between epoxy and TiO<sub>2</sub> nanogel composites (scheme 2b). Moreover, the formations of aggregated cluster with increment the TiO<sub>2</sub>-nanogel composite contents does not reduce the mechanical properties of epoxy films. This observation elucidates the formation of flexible nanogel networks improves the ability of epoxy coat to absorb both the abrasion and impact forces [36].

### 3.3. Salt spray of epoxy TiO<sub>2</sub> nanogel composites

The anticorrosion performance of epoxy coatings on steel substrate can be examined by salt spray resistance test as summarized in Table 4 and illustrated in Figure 6. The features the results are tested from the appearance of epoxy blistering and steel rust under epoxy films. The data confirm no osmotic blisters appeared in epoxy film even the blank but the rust more increased for blank film that was not blended with TiO<sub>2</sub> nanogel composites.

**Table 4.** Salt Spray Resistance of Cured epoxy TiO<sub>2</sub> nanogel composites.

TiO <sub>2</sub> nanogel	Nanogel content (Wt %)	Exposure time (Hours)	Disbonded area %	Rating Number (ASTM D1654)
TiO <sub>2</sub> -APTAC/AMPS- Na	0.1%	1000	1	9
	1%	750	50	2
	3%	500	60	1
TiO <sub>2</sub> -APTAC/AA	0.1%	1000	5	7
	1%	750	50	2
	3%	500	60	1
TiO <sub>2</sub> -APTAC/NIPAm	0.1%	1000	20	5
	1%	1000	10	6
	3%	500	60	1

The data (Table 4 and Figure 6) elucidate that the epoxy embedded with TiO<sub>2</sub>-APTAC/AMPS-Na (0.1 Wt %) achieved high salt spray resistance for 1000 h than other composites. This can be referred to the higher dispersion efficiency of TiO<sub>2</sub>-APTAC/AMPS-Na (0.1 Wt %) into epoxy matrix forms protective film at the epoxy surfaces prevents the diffusion of water or salts to react with steel surfaces. The negative surface charge (-33 mV) and particle size (93 nm) increase the interaction between TiO<sub>2</sub>-APTAC/AMPS-Na (0.1 Wt %) and epoxy matrix and hence their protection properties

increased. The  $\text{TiO}_2$ -APTAC/AMPS-Na nanoparticles possess unique protective characteristics properties produced from the large fraction of atoms that reside at the surface leading to strong interfacial interactions with the epoxy matrix [37-43].

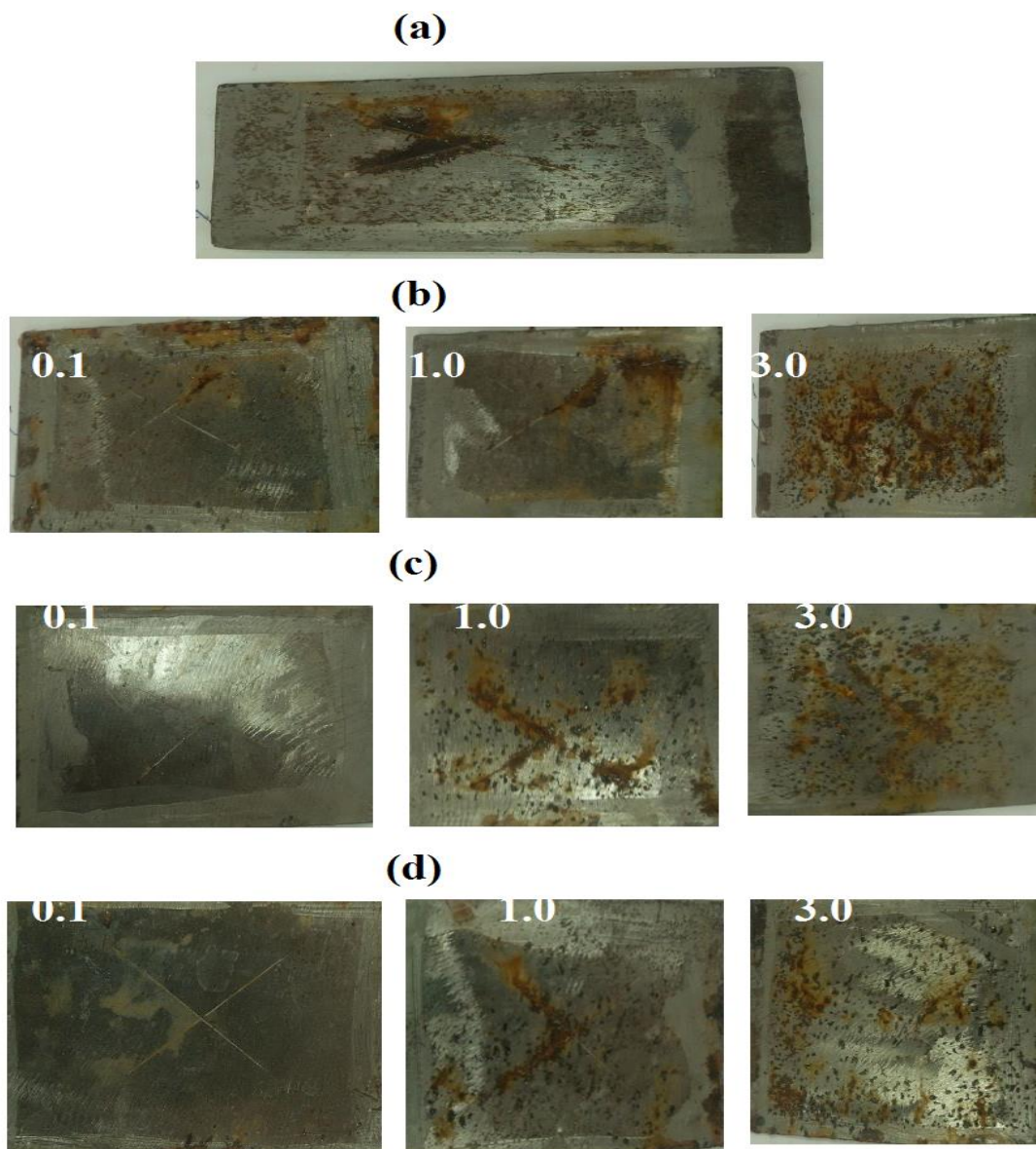


**Figure 6.** Salt spray resistance photos of cured epoxy resin embedded with different concentrations of a) blank, b)  $\text{TiO}_2$ -APTAC/NIPAm, c)  $\text{TiO}_2$ -APTAC/AMPSA-Na and d)  $\text{TiO}_2$ -APTAC/AA nanogel composites.

The increment of  $\text{TiO}_2$ -APTAC/AMPS-Na and  $\text{TiO}_2$ -APTAC/AA contents can form aggregates that affect the epoxy film texture and facilitate the salt and water diffusion into epoxy films. The data also confirm that the increment of  $\text{TiO}_2$  nanogel composites up to 1 Wt % reduces the salt spray resistances except  $\text{TiO}_2$ -APTAC/NIPAm which showed medium resistivity to salt spray resistance due to their low particle size of 65 nm (Table 2) facilitate the dispersability at high concentration. In case

of low concentration of TiO<sub>2</sub>-APTAC/NIPAm, the particles arranged themselves in the interstices positions and produced spaces to act as route for slipping of salt and water molecules to diffuse through the cured film [44]. Increment of TiO<sub>2</sub>-APTAC/NIPAm contents produce a more close-pack epoxy film texture and better corrosion inhibition can be detected [43]. The unmodified TiO<sub>2</sub> nanoparticles were not used in this work due to their very low dispersability in epoxy matrix.

Careful inspection of data represented in Figure 6 proves that both TiO<sub>2</sub>-APTAC/AMPS-Na and TiO<sub>2</sub>-APTAC/AA at low content can act as self-healing materials at low concentrations. It was noticed that no rust formed at X-cut as appeared in Figure 6 c and d using low TiO<sub>2</sub> nanogel content (0.1 Wt %). This behavior can be referred to the high salt resistivity of AMPS-Na and AA assists to increase the diffusion of nanoparticles at X cut (defected area). This observation was not observed in TiO<sub>2</sub>-APTAC/NIPAm (Figure 6 b). This behavior can be attributed to that the presence TiO<sub>2</sub>-APTAC/NIPAm ( polyelectrolyte) at defect area can act as conducting paths to increase , the electrochemical reactions at defected area to produce activated corrosion cell at steel surface to produce metal/oxide rusts [45, 46].

#### 4. CONCLUSIONS

TiO<sub>2</sub> nanoparticles as core can be encapsulated into polyampholyte or polyelectrolyte nanogel as core based on positively charged APTAC monomer using core/shell morphology. The correlation between particle sizes (nm) and zeta potential of TiO<sub>2</sub> nanogel composites concluded that their surface charges increased with increment of their particle sizes as confirmed for TiO<sub>2</sub>- APTAC/AMPS-Na which has particle size of  $93.0 \pm 15$  nm and zeta potential of  $-33.13 \pm 5$  mV. The surface charge values are increased in the direction of TiO<sub>2</sub>- APTAC/AMPS-Na > TiO<sub>2</sub>- APTAC/AA > TiO<sub>2</sub>-APTAC/NIPAm which have the same order of lowering particle sizes. The high surface charged particles based on TiO<sub>2</sub>- APTAC/AMPS-Na showed better corrosion resistance due to their surface charges assist them to increase the dispersion of particles into epoxy coatings and enhance the adhesion force of films to steel substrate. Therefore, it can be concluded that the increment of nanogel layer thickness on the titanium dioxide surfaces increases the surface charges of composite to achieve better corrosion protection performance.

#### ACKNOWLEDGEMENTS

The authors extend their appreciation to the Deanship of Scientific Research at King Saud University for funding this work through research group no RGP- 235.

#### References

1. C.A. May, G.Y. Tanaka, Epoxy resin chemistry and technology. New York: Marcel Dekker, (1973).
2. R.S. Baur, Epoxy resin chemistry, advances in chemistry. Washington (DC):American Chemical Society, 144 (1979).
3. W. G. Potter, Epoxide resins. New York: Springer, 77(1970).



4. L.V. Adams, J. A.Gannon, Encyclopedia of polymer science and engineering, New York: Wiley Interscience, (1986) 322-348.
5. R. Rahul, R. Kitey, *Compos. Part B Eng.*, 85 (2016) 336-342.
6. M. S. Goyat, S. Ray, P.K. Ghosh, *Compos. Part A Appl. Sci.*, 42(10) (2011) 1421-1431.
7. S. Halder, P. K. Ghosh, M. S. Goyat, S. Ray, *J. Adh. Sci. Technol.*, 27(2) (2013)111-124.
8. P. K. Ghosh, A. Pathak, M. S. Goyat, S., *J. Reinf. Plast Compos.*, 31(17) (2012)1180-1188.
9. S. Halder, P. K. Ghosh, M. S. Goyat, *Polymer*, 24(4) (2012)331-341.
10. J. L. H. Chau, C. T. Tung, Y. M. Lin, A. K. Li, *Mater. Lett.*, 62(19) (2008) 3416-3418.
11. X. Chen, S. S. Mao, *Chem. Rev.*, 107(7) (2007) 2891-2959.
12. W. Zhai, Z. M. Wu, X. Wang, P. Song, Y. He, R. M. Wang, *Prog. Org. Coat.*, 87(2015)122-128.
13. B. Wetzel, P. Rosso, F. Hauptert, K. Friedrich, *Eng. Fract. Mech.*, 73(16) (2006) 2375-1298
14. D. Olmos, C. Dominguez, P. D. Castrillo, J. Gonzalez-Benito, *Polymer*, 50(2009) 1732.
15. B. Bittmann, F. Hauptert, A. K. Schlarb, *Ultraso. Sonochem.*, 18(1) (2011)120-126.
16. B. Bittmann, F. Hauptert, A. K. Schlarb, *Ultraso. Sonochem.*, 16(5) (2009) 622-628.
17. A. Chandra, Turng, L. S. P. Gopalan, R. M. Rowell, S. Gong, *Compos. Sci. Technol.*, 68(3-4) (2008)768-776.
18. D. N. Bikiaris, A. Vassiliou, V. Pavlidou, G. P. Karayannidis, *Euro. Polym. J.*, 41(9) (2005)1965-1978.
19. M. Z. Rong, M. Q. Zhang, Y. X. Zheng, H. M. Zeng, R. Walter, K. Friedrich, *Polymer*, 42(1) (2001) 167-183.
20. T. S. Radoman, J. V. Dzunuzovic, K. B. Jeremic, B.N. Grgur, D. S. Milicevic, I. G. Popovic, *Mat. Des.*, 62(2014) 158-167.
21. X. Hu, E. Su, B. Zhu, J. Jia, P. Yao, Y. Bai, *Compos. Sci. Technol.*, 97 (2014) 6-11.
22. J. P. Holmberg, E. Ahlberg, J. Bergenholtz, M. Hassell, Z. Abbas, *J. Coll. Interf. Sci.*, 407 (2013) 168-176.
23. A. M. Atta , H. A. Al-Lohedan, A. M. Tawfeek, A. A. Abdel-Khalek, *Digest J. Nanomat. Biostr.*, 11(2016) 91 – 104.
24. G. A. El-Mahdy, A. M. Atta, H. A. Al-Lohedan, A. M. Tawfeek, A. A. Abdel-Khalek, *Int. J. Electrochem. Sci.*, 10 (7) (2015) 5702-5713.
25. M. Molina, M. Asadian-Birjand , J. Balach, J. Bergueiro , E. Miceli, M. Calderón, *Chem. Soc. Rev.*, 44 (2015) 6161-6186.
26. P. Thoniyot, M. J. Tan, A. Abdul Karim, D. James Y. X. J. Loh, *Adv. Sci.*, 2 (2015) 140.
27. Q. Song, , S. Cao, R. H. Pritchard, , B. Ghalei, , S. A. Al-Muhtaseb, , E. M. Terentjev, A. K. Cheetham, E. Sivaniah, *Nature Communications*, 5 (2014) 4813. doi:10.1038/ncomms5813
28. W. H. De Jong, P. J. A. Borm, *Int. J. Nanomedicine*, 3(2) (2008) 133-149.
29. H. S. Bae, M. K. Lee, W.W. Kim, C. K. Rhee, *Coll. Surf. A: Physiochem. Eng. Aspects*, 220 (2003) 169-177.
30. M. Ranka, P. Brown, and T. Alan Hatton, *ACS Appl. Mater. Interfaces*, 7 (35) (2015) 19651-19658.
31. J. C. Yu, L. Z. Zhang, Z. Zheng, J. C. Zhao, *Chem. Mater.*, 15 (2003) 2280
32. B. X. Du, J. W. Zhang, Y. Gao, *IEEE Trans. Dielect. Elect. Insul.*,19(3) (2012) 755-762 .
33. X. Z. Zhang, F. H. Wang, Y. L. Du, *Surf. Coat. Technol.*, 201 (2007) 7241-7245.
34. X. Z. Zhang, Y. J. Li, *Kem. Ind.*, 63 (9-10) (2014) 317-322
35. B. X. Du, J. W. Zhang and Y. Gao, *IEEE Trans. Dielect. Elect. Insul.*, 19(3) (2012)755-762.
36. R. G. Chaudhuri, S. Paria, *Chem. Rev.*, 112 (4) (2012)2373-2433.
37. A. K.Guin, S. K. Nayak, T. K. Rout, N. Bandyopadhyay, D. K. Sengupta, *J. Coat. Technol. Res.*, 9 (1) (2012) 97-106.
38. N. N. Voevodin, V. N. Balbyshev, M. Khobaib, M. S. Donley, *Prog. Org. Coat.*, 47 (4) (2003) 416-423.

39. A.M.K. Kirubaharan, M. Selvaraj, K. Maruthan, D. Jeyakumar, *J. Coat. Technol. Res.*, 9 (2) (2012) 163-170.
40. D. Vesely, A. Kalendova, *Prog. Org. Coat.*, 62 (1) (2008) 5-20.
41. C.R. Hegedus, I.L. Kamel, *J. Coat. Technol.*, 65 (822) (1993) 37-43.
42. M.Z. Rong, M.Q. Zhang, Y.X. Zheng, H. M. Zeng, R.Walter, K. Friedrich, *Polymer*, 42 (1) (2001) 167-183.
43. V. Barranco, Jr. S. Feliu, S. Feliu, *Corros. Sci.*, 46 (9) (2004) 2221-2240.
44. N. M. Ahmed, M.M. Selim, *Pigment & Resin Technol.*, 40 (1) (2011) 4-16.
45. B. Del Amo, R. Romagnoli, V.F. Vetere, *Ind. Eng. Chem., Res.* 38 (3) (1999)2310-2314.
46. Y. Shao, C. Jia, G. Meng, T. Zhang, F. Wang, *Corros. Sci.*, 51 (1) (2009) 371-379.

© 2017 The Authors. Published by ESG ([www.electrochemsci.org](http://www.electrochemsci.org)). This article is an open access article distributed under the terms and conditions of the Creative Commons Attribution license (<http://creativecommons.org/licenses/by/4.0/>).